3D modeling of aflibercept transport in the vitreous humor

Keywords: aflibercept, macular degeneration, VEGF, vitreous humor, COMSOL
BEE/MAE4530: Computer Aided Engineering: Applications to Biological Processes
Kevin Li, Matthew Limjoco, Jason Zarate

May 11, 2017

Contents

1 Executive Summary

Aflibercept is an anti-vascular endothelial growth factor (anti-VEGF) drug used to treat several retinal diseases such as macular degeneration. It accomplishes this by binding and inhibiting VEGF, which is the growth factor that is responsible for abnormal blood vessel growth. Overexpression of VEGF can lead to interference with the macula, and subsequent vision loss. Aflibercept is prescribed to treat macular degeneration due to VEGF overexpression. It is administered via intravitreal injection. Analysis of the transport of aflibercept through the vitreous humor is critical to understanding whether or not patients are receiving appropriate amounts of drug at the macula boundary, where the abnormal growth of blood vessels is contributing to macular degeneration. This study will assess if if the current market dose of aflibercept is successfully inhibiting VEGF for an appropriate time period.

The scope of analysis involved construction of a three-dimensional geometry of the vitreous humor in COMSOL, an implementation of physical properties and parameters of the vitreous humor and aflibercept, an illustration of key results, a sensitivity analysis on certain parameters, and a validation of the COMSOL implementation.

The analysis was conducted for a 3D diffusion problem, coupled with convection. Convection is due to pressure-driven flow, a result of the inherent pressure difference in the vitreous humor. Degradation or inactivation of aflibercept was also considered by modeling the second-order binding of aflibercept to VEGF.

The distribution of aflibercept throughout the vitreous humor was successfully determined. Due to asymmetry in the injection site, or the placement of drug, it was found that the distribution of drug is asymmetric at early times, and becomes more uniform at later times. A similar result was found at the macula boundary, which is the target area of interest for this study. It was also shown that VEGF concentration is successfully inhibited upon the introduction of aflibercept. Based on the model, VEGF began to accumulate after initial suppression within 20 to 40 days of aflibercept injection. This coincides with the recommended interval between aflibercept injections, which is 28 days.

Improvements in future model implementation could provide a result that more accurately represents the transport of aflibercept in the eye. These improvements include implementing an initial injection velocity when aflibercept is introduced, and the use of a more realistic geometry, such as an MRI scan, to build the geometry in the COMSOL model.

2 Introduction

A suite of retinal diseases, namely, 1) wet age-related macular degeneration, 2) diabetic macular edema, 3) diabetic retinopathy, and 4) macular edema following retinal vein occlusion, may be treated with aflibercept, an FDA-approved anti-VEGF prescription medication. The medium through which aflibercept is transported is the vitreous humor, a gelatinous body with well-studied properties. However, differing concentrations of aflibercept can have varying effects on the human eye. The ability to model such transport could help determine optimal levels of aflibercept for treatment of a multitude of retinal diseases. For proper treatment of many retinal diseases, the concentration of the treatment molecule must be kept at a constant level. Like other forms of macular treatment, aflibercept also degrades within the eye and the ability to model concentrations, as well as transport in three-dimensional space, is definitely advantageous. This will allow for optimization of drug injection as well as the minimization of injections, which itself can have many problems for the patient including optical discomfort and physical damage from the injection process. Such a model could also be useful in augmenting the drug development process by reducing dependence on clinical trials, which can be costly and invasive, due to the necessary injection of drug in the eye.

Several studies have delved into the nature of aflibercept administration and its optimal usage. Ohr and Kaiser's study of aflibercept injection on macular degeneration determined that dosages of 2 mg and 4 mg have proven to have significant improvement in vision at 8 week injections over 12 months. Aflibercept was the drug of choice as compared to other drugs used to treat retinal diseases, because it had a longer half-life within the eye as well as a higher binding affinity to VEGF. A variety of other studies have reported results on the geometry and the specific quantities of permeability and diffusivity of the eye. Other studies have modeled drug transport within the intravitreal fluid and have determined that the transport has both convective and diffusive components.

Current studies on treatment of macular degeneration have included three-dimensional coupled convective-diffusive transport of drugs through the usage of an implant that released drug at specified intervals [8]. Other studies include two-dimensional modeling of intravitreal injections within the eye with no adherence

to any single drug nor any vitreous substitutes [5]. Lastly, three-dimensional modeling specifically for aflibercept transport has not been done.

This study modeled aflibercept transport in three-space to address the need for three-dimensional intravitreal studies that are lacking in literature. It was also designed as a method to verify aflibercept effectiveness, with the hope of reducing dependence on clinical trials that can be costly and invasive. The model focused on the effects of diffusion, convection, and degradation on aflibercept transport, and the subsequent effects on VEGF.

2.1 Problem Statement

The purpose of this research was to model the transport of aflibercept in the vitreous humor and to analyze the effects of aflibercept on VEGF concentration over time. By doing so, it can be determined if aflibercept is inhibiting VEGF for a long enough time period. The model was constructed as a 3D diffusion problem, coupled with convection. This convection is due to pressure driven flow, which results from a pressure gradient within the vitreous humor. Degradation and production terms were also considered for both aflibercept and VEGF.

2.2 Design Objectives

The primary goal of this model was to determine if the current market concentration of aflibercept is sufficiently inhibiting VEGF for an appropriate time period. A COMSOL model was used to illustrate the distribution of drug throughout the vitreous humor, and analyze the effects of aflibercept on VEGF accumulation. The geometry, dimensions, and physical properties of the human eye were implemented into the COMSOL model. The following objectives were completed during the process of this study:

1. Constructed a 3D model in COMSOL that illustrates the geometry, dimensions, and physical properties of the human eye
2. Assessed the distribution of aflibercept throughout the vitreous humor over time, in addition to the distribution of aflibercept at the macula boundary over time
3. Identified parameters that have a large impact on aflibercept concentration at the macula boundary
4. Checked the validity of the model, with respect to aflibercept half-life in the vitreous humor, by comparing with literature
5. Determined the effects of aflibercept on VEGF concentration over time

3 System Geometry

Constructing a model in COMSOL requires proper implementation of geometry. Dimensions for the model constructed in COMSOL are taken from actual measurements of the human eye [2]. Assumptions were made where appropriate to simplify the model and reduce the total amount of computation needed. Such assumptions are discussed in section 3.2.

3.1 Physical Problem

In this study, the transport of aflibercept in the vitreous humor was modeled. Aflibercept is placed into the vitreous humor via intravitreal injection. Considering the eye to be oriented so that the pupil is facing upwards (Figure 1), a typical intravitreal injection site is located 3.5 mm posterior to the limbus and 5.5 mm to either the left or right of the pupil axis [12][2] (Figure 2). The injection site was modeled as a sphere with a radius of 2.285 mm, which was determined from the recommended dosage volume of 0.5 mL [1]

Figure 1: Illustration of the human eye during the intravitreal injection process. Drug is injected into the vitreous humor and transported throughout the eye through diffusion and pressure driven flow. The target area for aflibercept, an anti-VEGF drug, is a region of abnormal blood vessels adjacent to the macula that result from overexpression of VEGF.

Three-dimensional drug diffusion was modeled for aflibercept once it was injected into the vitreous humor. Aflibercept was modeled with first order metabolism and second order inactivation, due to the formation of an aflibercept-VEGF complex. Drug diffusion was coupled with convection, which is illustrated by Darcy's Law, and is caused by an inherent pressure gradient between the anterior hyaloid membrane and the posterior retina.

3.2 Schematic

The physical problem described in section 3.1 was converted to a schematic that could be used to construct the COMSOL model. Dimensions of the human eye, found in literature, were used to design the schematic (Table 1). Where appropriate, assumptions were made to simplify the model and reduce the total amount of computation needed.

Table 1: Dimensions of the human eye. Each value was found in literature and implemented in the geometry of the COMSOL model, as shown in Figure 2.

Dimension	Value (*mm*)	Source
Anterior hyaloid membrane radius	5.5	[2]
Distance between limbus and injection site	3.5	[12]
Radius of spherical injection site	2.285	[1]
Radius of vitreous humor	11	[2]
Distance between macula boundary and retina	0.425	[13]
Diameter of macula	5.5	[13]

The eye was assumed to be a perfectly round sphere, with a uniform radius in all directions. The lens of the eye, however was not considered in the schematic due to its impermeability. This is shown as a zero flux boundary condition at the anterior hyaloid membrane (denoted in red) which is approximated as a plane parallel to the surface of the pupil.

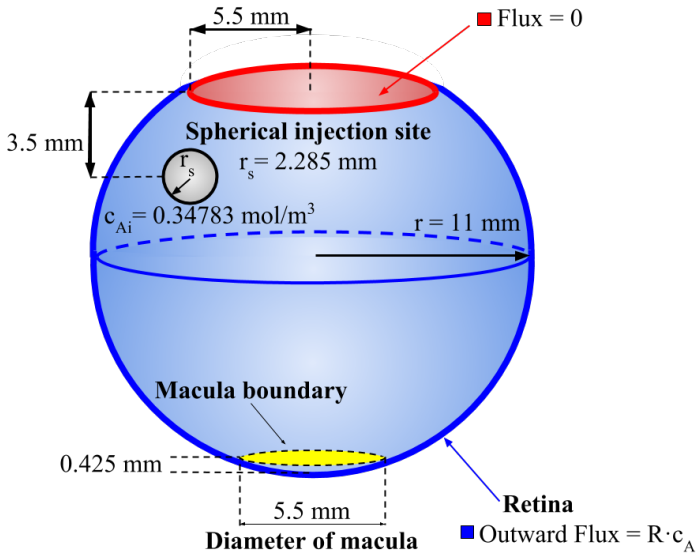

Figure 2: Schematic of the physical problem. Dimensions of the human eye, as found in literature, are indicated on the schematic. Boundary and initial conditions are also shown. There is no mass flux at the hyaloid membrane, shown in red. Throughout the retinal surface, shown in blue, there is an outwards flux condition, referred to as retinal clearance. The placement of drug in the vitreous humor after intravitreal injection is modeled as a small sphere with radius radius, r_s, and with initial concentration, c_{Ai}.

Specified boundary and initial conditions are shown in Figure 2. For more information on boundary and initial conditions, see section 5. At the hyaloid membrane (denoted in red) there is no flux. However, throughout the retinal surface (denoted in blue) there is an outwards flux condition, described in literature as retinal clearance [5]. The injected drug is modeled as a sphere of radius, r_s, with an initial concentration, c_{Ai}.

An additional schematic was designed to illustrate pressure-driven flow in the vitreous humor (Figure 3). Pressure-driven flow results from an inherent pressure gradient between the anterior hyaloid membrane and the posterior retina [5].

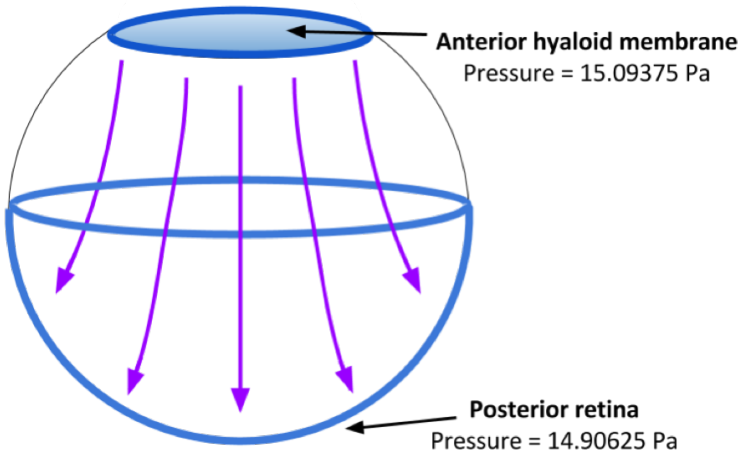

Figure 3: Additional schematic to show pressure-driven flow in the vitreous humor. Pressure difference between the anterior hyaloid membrane and the posterior retina results in flow. The velocity that results from this flow is calculated using Darcy's Law.

Higher pressure is exhibited at the anterior hyaloid membrane and lower pressure is exhibited at the posterior retina [5]. This difference in pressure results in flow within the vitreous humor towards the posterior retina. This pressure-driven flow is implemented in the model using Darcy's Law (see section 4).

4 Governing Equations

The physics of the problem needs to be described in the form of governing equations. This model uses governing equations for two species: aflibercept and VEGF. Listed below are equations that govern the transport, degradation, and production of aflibercept and VEGF.

Equation 1 is the governing equation for aflibercept transport.

$$\frac{\partial c_A}{\partial t} + (u_x \frac{\partial c_A}{\partial x} + u_y \frac{\partial c_A}{\partial y} + u_z \frac{\partial c_A}{\partial z}) = D_A(\frac{\partial^2 c_A}{\partial x^2} + \frac{\partial^2 c_A}{\partial y^2} + \frac{\partial^2 c_A}{\partial z^2}) + r_V + r_A \tag{1}$$

It contains a transient term, a convective term, a diffusive term, a second order inactivation term, r_V, and a first order metabolism term, r_A. Velocities, u, in the convective term are calculated using Darcy's Law (Equation 6). The diffusion term is governed by the diffusion coeffient, D_A.

The governing equation for VEGF is given by Equation 2.

$$\frac{\partial c_V}{\partial t} + (u_x \frac{\partial c_V}{\partial x} + u_y \frac{\partial c_V}{\partial y} + u_z \frac{\partial c_V}{\partial z}) = D_V(\frac{\partial^2 c_V}{\partial x^2} + \frac{\partial^2 c_V}{\partial y^2} + \frac{\partial^2 c_V}{\partial z^2}) + r_V + r_P \tag{2}$$

Similar to the aflibercept governing equation, the governing equation includes a transient term, a convective term, a diffusive term, and a second order inactivation term. Velocities, obtained from Darcy's Law (Equation 6), are calculated in the same way as for Equation 1. The diffusion term for VEGF is governed by the diffusion coefficient, D_V.

The inactivation term, r_V, which depends on both the concentration of free aflibercept, c_A, and VEGF, c_V, is defined by Equation 3 with a second order rate constant, k_V.

$$r_V = -k_V \cdot c_A \cdot c_V \tag{3}$$

This second order inactivation is due to the formation of an aflibercept-VEGF complex, which essentially renders both species inactive. The inactivation term, r_V, is present in both Equation 1 and Equation 2. This is because both aflibercept and VEGF are involved in forming the aflibercept-VEGF complex.

The first order metabolism term, r_A, is defined by Equation 4 and contains the first order rate constant k_A.

$$r_A = -k_A \cdot c_A \tag{4}$$

Equation 4 describes the degradation of aflibercept in the vitreous humor. No studies have been conducted on the exact mechanicisms of aflibercept metabolism but is expected to undergo metabolism via proteolysis [1]

Zeroth order production of VEGF, r_P, is considered in the model and is governed by the rate constant, k_P.

$$r_P = k_P \tag{5}$$

Rate constants and parameters specified in the governing equations are discussed further in section 6.

Darcy's Law is implemented in the model at steady-state.

$$u = -\frac{K}{\mu}\nabla P \tag{6}$$

Darcy's Law requires the following properties: permeability, K, vitreous humor viscosity, μ, and pressure gradient, ∇P.

5 Boundary and Initial Conditions

Boundary and initial conditions are a necessary part of any mass transfer problem. Without them, it is impossible to find particular solutions within a domain for a given governing equation. The following boundary and initial conditions (Table 2) were found in literature and implemented in the COMSOL model.

Table 2: Boundary and Initial Conditions. Conditions that needed to be implemented in the model to solve the governing equations were found in literature. See the following text in section 5 for explanations of these conditions. For more details on the flux at the retina boundary, see section 6.

Boundary Condition	Value	Units	Source
Flux at hyaloid membrane	0	$\frac{mol}{m^2 \cdot s}$	[5]
Flux at the retina boundary	$R \cdot c_A$	$\frac{mol}{m^2 \cdot s}$	[5]
Pressure at hyaloid membrane	15.09375	Pa	[5]
Pressure at vitreous humor	14.90625	Pa	[5]
Initial drug concentration in vitreous humor	0	$\frac{mol}{m^3}$	N/A
Initial drug concentration in injection site	40	$\frac{mg}{mL}$	[1]
Initial drug concentration in injection site	0.34783	$\frac{mol}{m^3}$	[1]
Initial VEGF concentration	$1.3122 \cdot 10^{-7}$	$\frac{mol}{m^3}$	[9]
Initial pressure in vitreous humor	15	Pa	[5]

Boundary conditions of the vitreous humor domain, including flux at the hyaloid membrane, flux at the retina boundary, and pressure gradient in the eye, are adapted from models on two-dimensional intravitreal transport [5]. Pressure values were calculated to account for the 1.25% pressure drop in the vitreous humor. An average pressure of 15 Pa, as noted by Ferreira et al., was used as the mean pressure in the vitreous humor [5]. A 0.625% pressure difference between the vitreous humor and the posterior retina, and a 0.625% pressure difference between the anterior hyaloid membrane and the vitreous humor, were calculated, then subtracted from and added to the mean pressure, respectively. Initial drug concentration was obtained from the Eylea Full Prescribing Information (Regeneron Pharmaceuticals, Inc.). Initial VEGF concentration was obtained from Nonobe et al [9].

6 Input Parameters

Input parameters are also required to solve governing equations for mass transport. Like boundary and initial conditions, parameters are obtained from literature and implemented in the COMSOL model (Table 3).

Table 3: Input parameters. Justifications for each of the parameters chosen are explained in the following text and supported by sources.

Parameter	Symbol	Value	Units	Source
Drug diffusion coefficient	D_A	$5.556 \cdot 10^{-10}$	$\frac{m^2}{s}$	[5]
VEGF diffusion coefficient	D_V	$1.42 \cdot 10^{-10}$	$\frac{m^2}{s}$	[7]
Second order inactivation rate constant	k_V	$410 \cdot 10^{-5}$	$\frac{1}{M \cdot s}$	[10]
First order metabolism rate constant	k_A	$149.26 \cdot 10^{-9}$	$\frac{1}{s}$	[6]
Zeroth order production rate constant	k_P	$1.22 \cdot 10^{-14}$	$\frac{M}{s}$	[11]
Permeability in vitreous humor	K	$10 \cdot 10^{-17}$	m^2	[4]
Vitreous humor viscosity	μ	$1 \cdot 10^{-3}$	$Pa \cdot s$	[5]
Retinal clearance	R	$1 \cdot 10^{-9}$	$\frac{m}{s}$	[5]

Drug diffusion coefficient for aflibercept, D_A , was adapted from that of dexamethasone, an intravitreal corticosteroid [5]. VEGF diffusion coefficient, D_V, was obtained from Hutton-Smith et al [7].The second order inactivation rate constant, k_V , describes the binding of aflibercept and VEGF to form an aflibercept-VEGF complex. This value was obtained from Papadopoulos et al.[10]. Aflibercept degradation in the eye is governed by a first order metabolism rate constant, k_A , which was obtained from Finley et al. [6] VEGF production in the eye is governed by a zeroth order production rate constant, k_P [11]. Permeability in the vitreous humor, K, was derived from an intrinsic permeability value for meat [4]. The vitreous humor was treated as a permeating fluid with viscosity, μ [5]. Retinal clearance, R, is defined as the rate of clearance of drug at the retina boundary. This was implemented into the flux boundary condition at the retina (see section 5), which states that flux is dependent on concentration at the boundary [5].

7 System Discretization

In a computational software such as COMSOL, computations are only performed at certain nodes within the domain. To obtain values at different locations within the domain that are not nodes, interpolations are

performed. Error that results from interpolations is known as discretization error. To minimize this error, a more refined mesh could be used. However, more refined meshes require more computational time. The method for determining mesh is described in section 7.2.

7.1 Mesh

A mesh was defined for the system geometry in COMSOL (Figure 4).

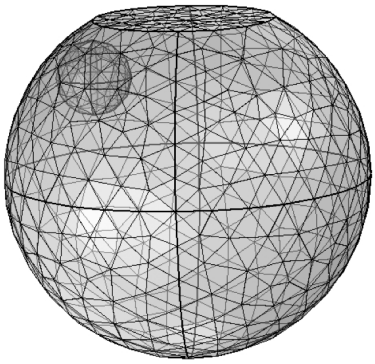

Figure 4: A user-defined mesh for the system geometry in COMSOL. The mesh configuration is given in Table 4

For the mesh configuration used, there was a total of 8855 domain elements, 1042 boundary elements, and 143 edge elements. The corresponding element parameters are shown in Table 4. To verify selection of mesh that gives both an acceptable solution, and reduces unnecessary computation time, a mesh convergence was performed, which is described in section 7.2 (Figure 5).

Table 4: Parameters of the mesh configuration used in COMSOL. The specified mesh configuration was chosen based on a mesh convergence analysis (section 7.2).

Element Parameter	Value
Maximum element size	$0.0022\ m$
Minimum element size	$3.96 \times 10^{-4}\ m$
Maximum element growth rate	1.5
Curvature factor	0.6
Resolution of narrow regions	0.5

From the mesh convergence in section 7.2, it was determined that the configuration shown in Table 4 is appropriate for the given problem; it limits spatial discretization error without taking up unnecessary computation time.

7.2 Mesh Convergence

A mesh convergence was performed to verify that spatial discretization error is kept at minimum. Four different mesh configurations (Figure 5) were implemented, and a plot of minimum concentration at the posterior retina vs. time was generated for each mesh. From the mesh convergence analysis, it was determined that the mesh configuration specified in Table 4, as illustrated by the green line, has a solution that converges with the dark blue line, which specifies a more refined mesh configuration.

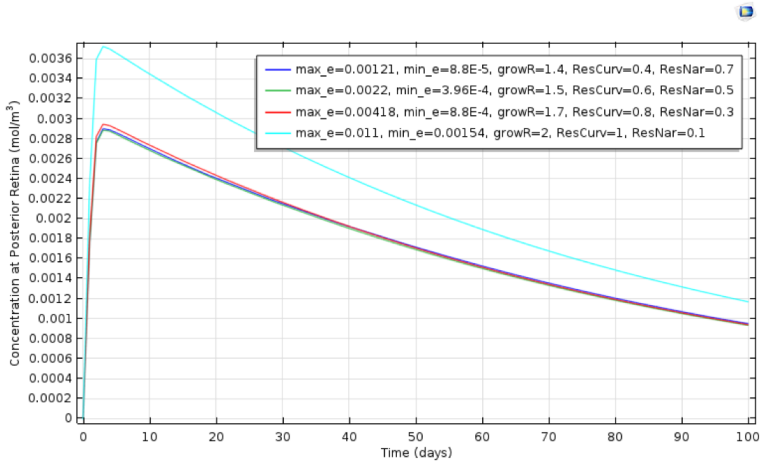

Figure 5: In this mesh convergence, the minimum concentration of drug at macular boundary was plotted over time for four different mesh configurations.

Table 5: Abbreviations for mesh convergence configuration parameters

Abbreviation	Parameter
max e	Maximum element size
min e	Minimum element size
growR	Maximum element growth rate
ResCurv	Curvature factor
ResNar	Resolution of narrow regions

The mesh configuration specified by the green line was chosen because unlike the red or teal line, it converges with the configuration specified by the dark blue line, which is for a finer mesh. Thus, the configuration used should have a limited discretization error, without taking up too much computation time.

8 Results

To visualize the distribution of aflibercept in the vitreous humor at various times, surface plots of the entire domain, as well as the macula boundary are shown.

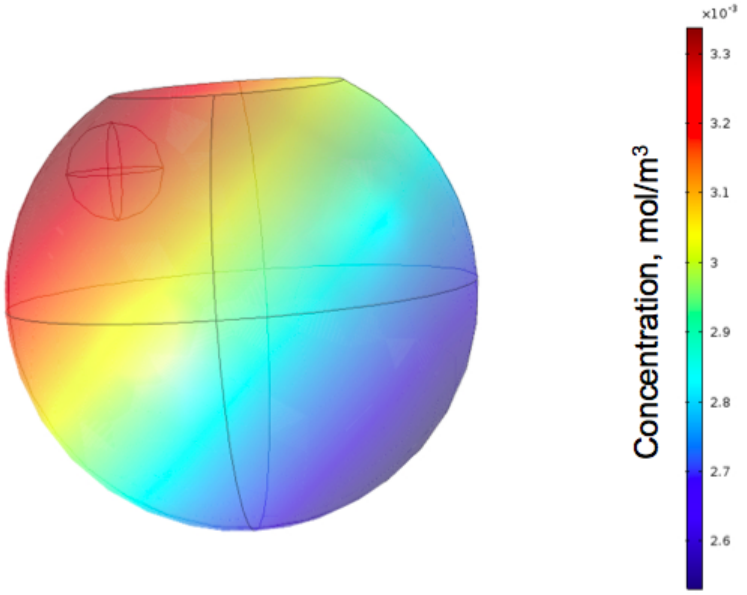

Figure 6: Surface plot at t = 1 day. It appears that after 1 day, the distribution of drug is asymmetrical and is dependent on the position of the injection site

As seen in Figure 6, the distribution of drug as asymmetrical. There is more drug concentrated in the vicinity of the injection sphere in comparison to the regions farthest from the injection sphere. This asymmetry at early times exhibits the value of using a three-dimensional model, since a two-dimensional axisymmetric model would not incorporate this slanted distribution of drug.

The typical time between injections of aflibercept is roughly 28 days. Therefore, a surface plot of aflibercept distribution after 28 days has elapsed is shown in Figure 7. This plot will give a better understanding of both the distribution and amount of drug at a time when another injection is expected.

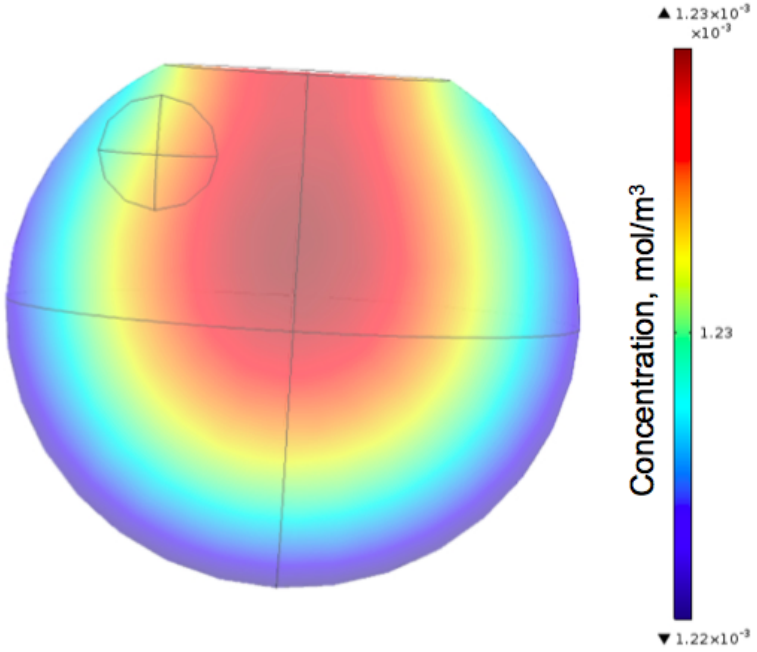

Figure 7: Surface plot at t = 28 days. Concentrations are virtually uniform at later times.

As seen in Figure 7, the distribution of drug is more symmetrical than the distribution of drug after 1 day has elapsed. This is expected, since enough time has passed allowing a distribution closer to equilibrium to be reached. However, it is also critical to note that there are very minute differences in concentration between the regions where concentration is highest and where concentration is lowest. Taking into consideration the scale of the surface plot shown in Figure 7, is clear that the minimum and maximum values are very close to each other, demonstrating this uniformity after long times.

Next, plots of the macula boundary are shown. To reiterate, the macula boundary is a two-dimensional slice of our model that is defined as a critical region of interest due to its proximity to the macula, the region where damage due to blood vessel proliferation is most detrimental. This is the area where concentrations of aflibercept should be adequately high, in order to inactivate appropriate amounts of VEGF.

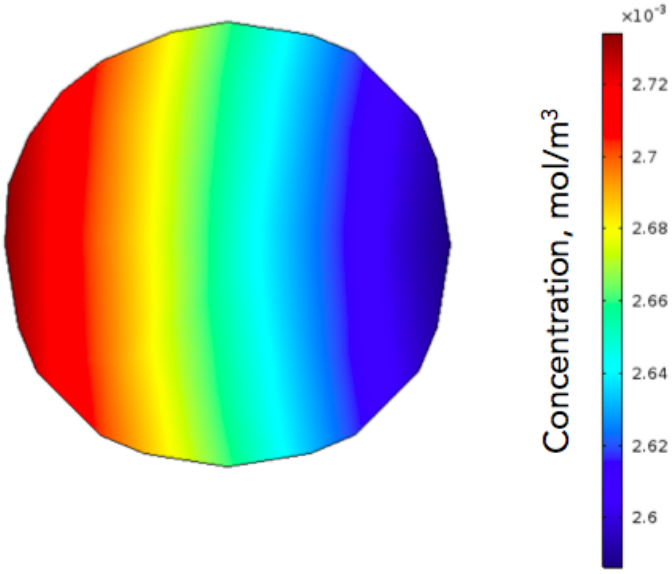

Figure 8: Surface plot of the macula boundary (see Figure 2 for exact location) at t = 1 day, which shows aflibercept concentration is concentrated on one side due to the asymmetry of this problem

Once again, Figure 8 demonstrates the value of a 3D model at early times, due to its asymmetry. As seen in the plot, there is a higher concentration of aflibercept on the left side in comparison to the right side, due to the initial placement of the injection sphere a distance away from the central axis.

Figure 9, like Figure 7, shows that aflibercept distribution approaches equilibrium after 28 days, which is the typical time between aflibercept injections.

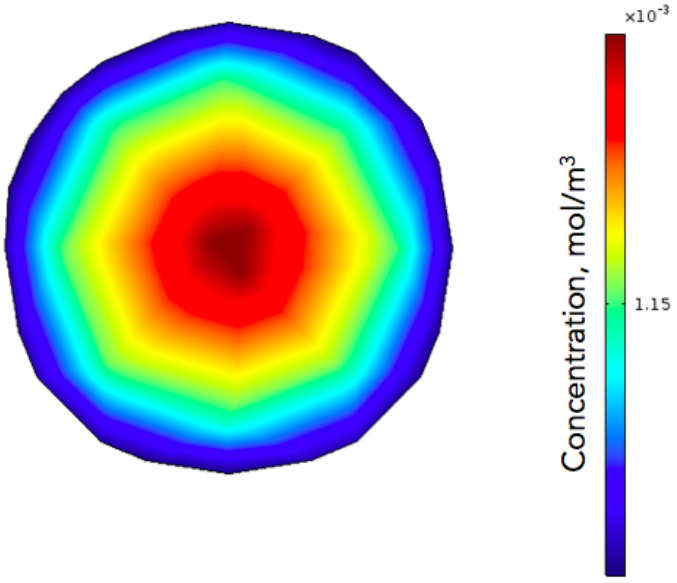

Figure 9: Surface plot of the macula boundary (see Figure 2 for exact location) at t = 28 day, which shows aflibercept concentration is roughly uniform after long times.

While the distribution appears symmetrical, it is once again important to note that the highest concentration in the plot is virtually equivalent to the lowest concentration in the plot.

Next, a visualization for pressure-driven flow was generated in COMSOL.

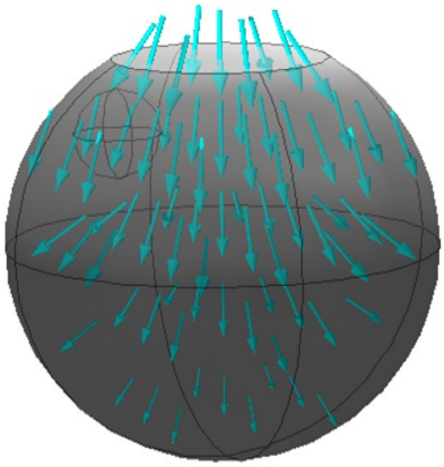

Figure 10: Velocity field in the vitreous humor due to pressure difference between the anterior hyaloid membrane and the posterior retina

The velocity field shows the direction and magnitude of flow in the model, which is the basis for the convective terms in the governing equations for both aflibercept and VEGF.

9 Validation

Validation for the model was done in terms of aflibercept half-life in the vitreous humor. Half-life is defined as the time at which the amount of drug in the vitreous humor is half of the initial amount injected. Since the initial concentration, in $\frac{mol}{m^3}$, is 0.34783, the initial amount of drug, in mol, is $1.73915 \cdot 10^{-8}\ mol$. Thus, half-life is the time at which the total amount of drug in the vitreous humor is $8.69575 \cdot 10^{-9}\ mol$. Taking into account the volume of the vitreous humor domain, the half life should occur when the average concentration is $0.0015 \frac{mol}{m^3}$.

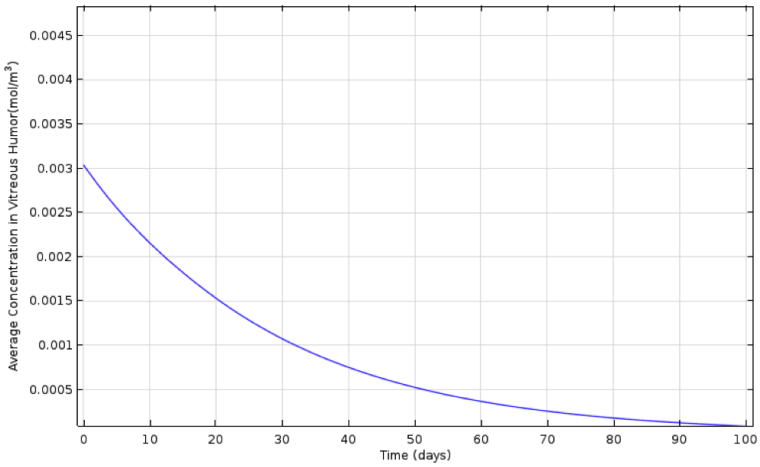

Figure 11: Plot of average concentration of aflibercept vs time. The time at which half of the total drug is taken away from the domain is roughly 20 days.

According to literature, an appropriate half-life for aflibercept is within the range of 4.5 and 4.8 days [3]. If the half-life in the model is within this range, then the model is roughly validated. The model showed a half-life of about 20 days, which is notably greater than values found in literature, but sensible considering that animal models were used to calculate shorter half lives while this model is intended for human eyes. Therefore, longer half lives determined in this model (due to human metabolism being slower than rabbit metabolism) are reasonable.

To validate this model further, concentrations of VEGF in the vitreous humor were observed (Figure 11). By taking into account the rate of change of VEGF at various times, as well as the typical amount of time between aflibercept injections, a more sensible reasoning for the results can be achieved.

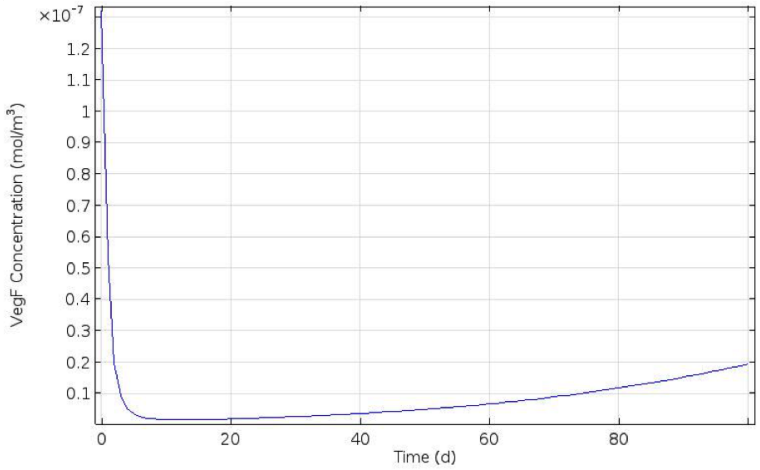

Figure 12: Plot of average concentration of VEGF vs time.

Figure 12, which plots the average concentration of VEGF in the vitreous humor over time, made clear that VEGF concentration drops significantly at early times as it binds to aflibercept and becomes inactivated via complex formation. After 28 days elapsed, the rate of change of VEGF began to increase due to zeroth order production, which is intuitive since it would be sensible to have another aflibercept injection if VEGF concentration begins to rise again (since there is already VEGF overexpression).

9.1 Sensitivity Analysis

A sensitivity analysis on five selected input parameters was performed (Figure 13). The selected parameters were initial drug concentration, diffusion coefficient of the drug, viscosity of vitreous humor, permeability of vitreous humor, and retinal clearance. A range approach was used, which involved changing each parameter of interest by $\pm 10\%$. The effect on the result, which is the minimum concentration of aflibercept at the macula boundary at 28 days, was observed for each parameter change. In a physical sense, the only parameters that can be altered are the initial drug concentration and the diffusion coefficient of the drug.

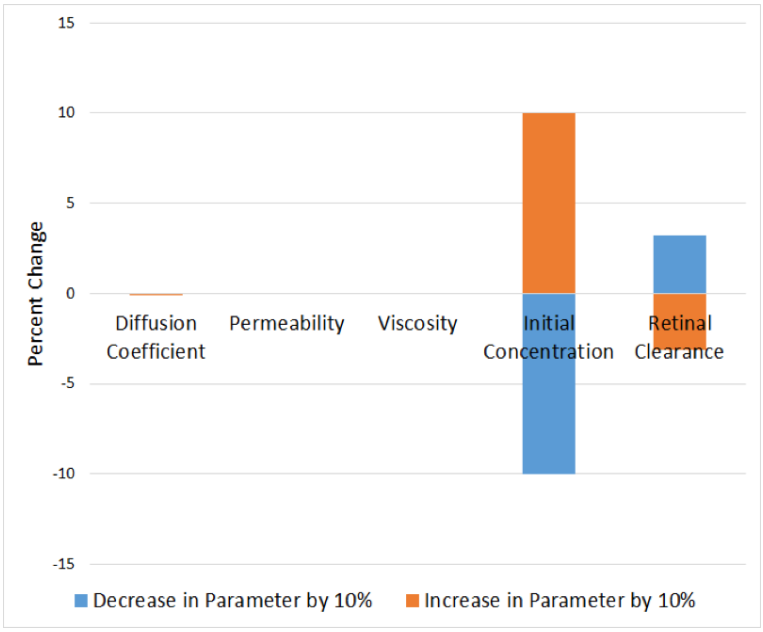

Figure 13: Sensitivity analysis for the following parameters: initial drug concentration, diffusion coefficient of the drug, viscosity of vitreous humor, permeability of vitreous humor, and retinal clearance.

The sensitivity analysis suggests that initial concentration of drug, and retinal clearance have the most impact on minimum drug concentration at the macula boundary. Diffusion coefficient, permeability, and viscosity have little to no impact.

10 Conclusions and Design Recommendations

The model described exhibits characteristics mirroring the intravitreal injection procedure. A three-dimensional model was successfully constructed, which is a significant improvement over the two-dimensional models and two-dimensional axisymmetric models commonly found in literature. With respect to more specific results, it was found that asymmetric drug distributions were most apparent at early times in comparison to later times. At the macula boundary, this asymmetry was noted at earlier times too, where the inital position of the injection sphere played a major role on the appearance of the surface plot. Validation was achieved in two ways: by comparing half-life with values found in literature, and by noting the amount of time between aflibercept injections while considering amounts of VEGF at various times. These comparisons assure that the model is computing concentrations with reasonable accuracy. Furthermore, it is recommended that the time between aflibercept injections remain at 28 days.

Theoretically, the model could be utilized to model the transport of other drugs administered the same way. Moreover, this study sheds light upon which input parameters influence the results the most. In this study, it was found that these particular parameters were initial concentration and retinal clearance. The model has important implications in the field of biotechnology as it can provide supporting data for drugs in the clinical trial phase. Such models allow drug developers to gain insight regarding the behavior of intravitreal drugs without having to spend as much money on physical experiments and additional research. Ultimately, the usage of models similar to the one proposed in this study will lead to great savings and a more comprehensive understanding of real-world problems.

Further improvements to this model that would result in potentially more accurate and realistic results. One improvement could be the use of a more realistic geometry. This could be achieved by importing more detailed meshes or scans, such as an MRI, from online databases. Another improvement that could be made is including convection as a result of the injection process. Including the injection in the model as opposed to an injection sphere with an initial concentration would be more realistic than the current model.

References

[1] Eylea full prescribing information, 2016.

[2] Gabriela Apiou-Sbirlea and Jean P. L'huillier. Simulation and optimization of argon laser iridectomy: influence of irradiation duration on a corneal and lens thermal injury. *Medical Applications of Lasers in Dermatology, Cardiology, Ophthalmology, and Dentistry II*, Sep 1998.

[3] John B. Christoforidis, Michelle M. Williams, Shankaran Kothandaraman, Krishan Kumar, Frank J. Epitropoulos, and Michael V. Knopp. Pharmacokinetic properties of intravitreal i-124-aflibercept in a rabbit model using pet/ct. *Current Eye Research*, 37(12):1171–1174, 2012.

[4] Ashim K. Datta. [4530] permeability value for project, Mar 2017.

[5] J.a. Ferreira, Paula De Oliveira, P.m. Da Silva, and R. Silva. Mathematics of aging: Diseases of the posterior segment of the eye. *Computers & Mathematics with Applications*, 73(1):11–26, 2017.

[6] Sd Finley, P Angelikopoulos, P Koumoutsakos, and As Popel. Pharmacokinetics of anti-vegf agent aflibercept in cancer predicted by data-driven, molecular-detailed model. *Pharmacometrics and Systems Pharmacology*, 4(11):641–649, Oct 2015.

[7] Laurence A. Hutton-Smith, Eamonn A. Gaffney, Helen M. Byrne, Philip K. Maini, Dietmar Schwab, and Norman A. Mazer. A mechanistic model of the intravitreal pharmacokinetics of large molecules and the pharmacodynamic suppression of ocular vascular endothelial growth factor levels by ranibizumab in patients with neovascular age-related macular degeneration. *Molecular Pharmaceutics*, 13(9):2941–2950, May 2016.

[8] Jyoti Kathawate and Sumanta Acharya. Computational modeling of intravitreal drug delivery in the vitreous chamber with different vitreous substitutes. *International Journal of Heat and Mass Transfer*, 51(23-24):5598–5609, 2008.

[9] Norie Ito Nonobe, Shu Kachi, Mineo Kondo, Yoshiko Takai, Koji Takemoto, Atsushi Nakayama, Masahiro Hayakawa, and Hiroko Terasaki. Concentration of vascular endothelial growth factor in aqueous humor of eyes with advanced retinopathy of prematurity before and after intravitreal injection of bevacizumab. *Retina*, 29(5):579–585, 2009.

[10] Nicholas Papadopoulos, Joel Martin, Qin Ruan, Ashique Rafique, Michael P. Rosconi, Ergang Shi, Erica A. Pyles, George D. Yancopoulos, Neil Stahl, Stanley J. Wiegand, and et al. Binding and neutralization of vascular endothelial growth factor (vegf) and related ligands by vegf trap, ranibizumab and bevacizumab. *Angiogenesis*, 15(2):171–185, Feb 2012.

[11] Derek J Saunders, Philipp S Muether, and Sascha Fauser. A model of the ocular pharmacokinetics involved in the therapy of neovascular age-related macular degeneration with ranibizumab. *British Journal of Ophthalmology*, 99(11):1554–1559, May 2015.

[12] Caroll Shields and Fairoozp Manjandavida. The role of intravitreal chemotherapy for retinoblastoma. *Indian Journal of Ophthalmology*, 63(2):141, 2015.

[13] Robert G. Small. *The Clinical Handbook of Ophthalmology*. Parthenon Pub., 1997.

Appendix

Appendix A: Input parameters.

Parameter	Symbol	Value	Units	Source
Anterior hyaloid membrane radius	N/A	5.5	m	[2]
Curvature factor	ResCurv	0.6	N/A	COMSOL
Diameter of macula	N/A	5.5	m	[13]
Distance between macula boundary and retina	N/A	0.425	m	[13]
Distance between limbus and injection site	N/A	3.5	m	[12]
Drug diffusion coefficient	D_A	$5.556 \cdot 10^{-10}$	$\frac{m^2}{s}$	[5]
First order metabolism rate constant	k_A	$149.26 \cdot 10^{-9}$	$\frac{1}{s}$	[6]
Flux at hyaloid membrane	N/A	0	$\frac{mol}{m^2 \cdot s}$	[5]
Flux at the retina boundary	N/A	$R \cdot c_A$	$\frac{mol}{m^2 \cdot s}$	[5]
Initial drug concentration in injection site	N/A	40	$\frac{mg}{mL}$	[1]
Initial drug concentration in injection site	c_{Ai}	0.34783	$\frac{mol}{m^3}$	[1]
Initial drug concentration in vitreous humor	N/A	0	$\frac{mol}{m^3}$	N/A
Initial pressure in vitreous humor	N/A	15	Pa	[5]
Initial VEGF concentration	N/A	$1.3122 \cdot 10^{-7}$	$\frac{mol}{m^3}$	[9]
Maximum element size	max e	0.0022	m	COMSOL
Maximum element growth rate	growR	1.5	N/A	COMSOL
Permeability in vitreous humor	K	$10 \cdot 10^{-17}$	m^2	[4]
Pressure at hyaloid membrane	N/A	15.09375	Pa	[5]
Pressure at vitreous humor	N/A	14.90625	Pa	[5]
Minimum element size	min e	$3.96 \cdot 10^{-4}$	m	COMSOL
Radius of spherical injection site	r_s	2.285	m	[1]
Radius of vitreous humor	N/A	11	m	[2]
Resolution of narrow regions	ResNar	0.5	N/A	COMSOL
Retinal clearance	R	$1 \cdot 10^{-9}$	$\frac{m}{s}$	[5]
Second order inactivation rate constant	k_V	$410 \cdot 10^{-5}$	$\frac{1}{M \cdot s}$	[10]
VEGF diffusion coefficient	D_V	$1.42 \cdot 10^{-10}$	$\frac{m^2}{s}$	[7]
Vitreous humor viscosity	μ	$1 \cdot 10^{-3}$	$Pa \cdot s$	[5]
Zeroth order production rate constant	k_P	$1.22 \cdot 10^{-14}$	$\frac{M}{s}$	[11]

Appendix B. Computational time taken in an average run.

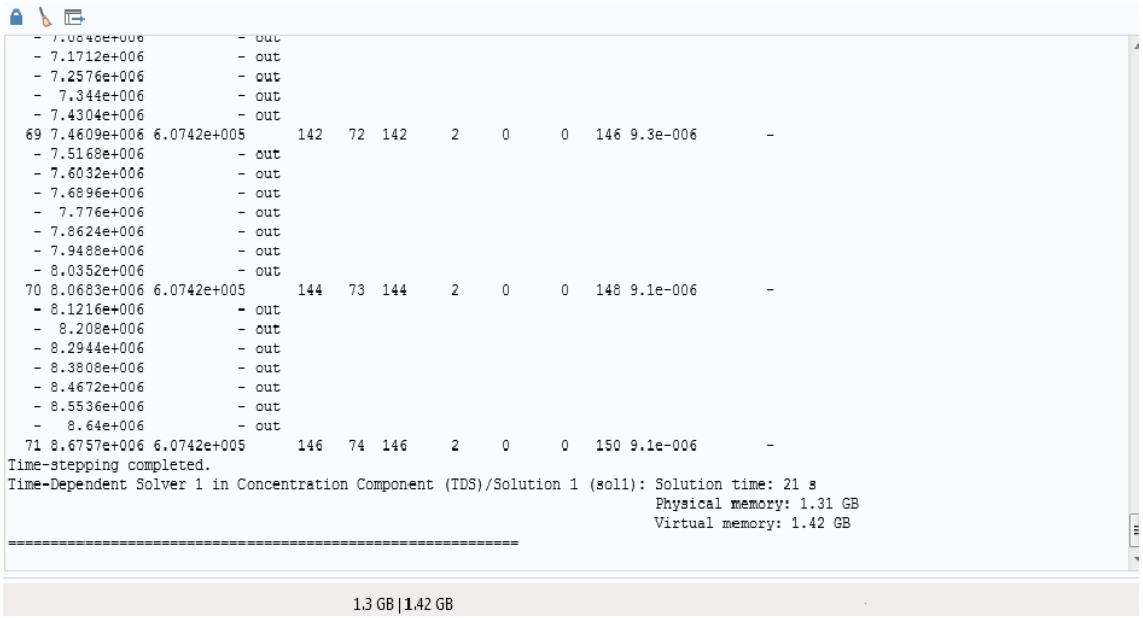

Figure 14: Computational time taken in an average run

Team member name	Member 1	Member 2	Member 3	Member 4	NOT DONE
Wrote abstract	X	X	X		
Edited abstract	X	X	X		
Wrote introduction	X	X	X		
Edited introduction	X	X	X		
Wrote method section	X	X	X		
Edited method section	X	X	X		
Wrote results section	X	X	X		
Edited results section	X	X	X		
Wrote discussion section		X			
Edited discussion section	X	X	X		
Wrote summary and conclusion section	X	X	X		
Edited summary and conclusion section	X	X	X		
Wrote bibliography section	X	X	X		
Edited bibliography section	X	X	X		
Prepared processed data table for appendix	X	X	X		
Checked data in processed data table in appendix	X	X	X		
Prepared figures or tables for main text	X	X	X		
Checked figures or tables in main text	X	X	X		
Assigned tasks to group members			X		
Put the report together from the parts provided by others	X	X	X		
Read and edited entire document to check for consistency	X	X	X		

Figure 15: Team Responsibilities